PAPER • OPEN ACCESS

Impact of Magnetic Focusing on the Transport of Energetic Electrons in the Solar Corona

To cite this article: Bofeng Tang et al 2023 J. Phys.: Conf. Ser. 2544 012004

View the article online for updates and enhancements.

You may also like

- Gyrosynchrotron Emission Generated by Nonthermal Electrons with the Energy Spectra of a Broken Power Law Zhao Wu, Yao Chen, Hao Ning et al.
- RADIOACTIVE POSITRON EMITTER PRODUCTION BY ENERGETIC ALPHA
 PARTICLES IN SOLAR FLARES R. J. Murphy, B. Kozlovsky and G. H.
- Ion Acceleration and the Development of a Power-law Energy Spectrum in Magnetic Reconnection
 H. Che, G. P. Zank and A. O. Benz

2544 (2023) 012004 doi:10.1088/1742-6596/2544/1/012004

Impact of Magnetic Focusing on the Transport of Energetic Electrons in the Solar Corona

Bofeng Tang^{1,2}, Haihong Che^{1,2}, Gary P. Zank^{1,2}

- 1 Department of Space Science, University of Alabama in Huntsville, Huntsville, AL 35899, USA
- ² Center for Space Plasma and Aeronomic Research (CSPAR), University of Alabama in Huntsville, Huntsville, AL 35805, USA

E-mail: bt0008@uah.edu, Haihong.Che@uah.edu,garyp.zank@gmail.com

Abstract. Observations of Type III radio bursts discovered that electron beams with power-law energy spectra are commonly produced during solar flares. The locations of these electron beams are ~ 300 Mm above the particle acceleration region of the photosphere, and the velocities range from 3 to 10 times the local background electron thermal velocity. However, the mechanism that can commonly produce electron beams during the propagation of energetic electrons with power-law energy spectra in the corona remains unclear. In this paper, using kinetic transport theory, we find for the first time that the magnetic focusing effect governs the formation of electron beams over the observational desired distance in the corona. The magnetic focusing effect can sharply increase the bulk velocity of energetic electrons to the observed electron beam velocity within 0.4 solar radii (300 Mm) as they escape from the acceleration region and propagate upward along magnetic field lines. In more rapidly decreasing magnetic fields, energetic electrons with a harder power-law energy spectrum can generate a higher bulk velocity, producing type III radio bursts at a location much closer to the acceleration region. During propagation, the spectral index of the energetic electrons is unchanged.

1. Introduction

Solar type III radio bursts, first discovered by Wild & McCready [1], are transient radio emissions drifting from higher frequencies to lower frequencies as a function of time. The type III radio bursts are commonly believed to be produced by propagating electron beams via an electron two-stream instability (ETSI) [2,3] as was proposed by Ginzburg & Zhelezniakov (1958) [4]. Recently discovered radio bursts showed that electrons beams are commonly produced in solar flares [5–7]. In particular, numerous nanoflare-associated radio bursts were discovered [8], implying that electron beams are distributed widely in the solar corona, and very probably contribute to the formation of the electron halo in the solar wind [9, 10]. However, the previous studies [5, 11] focus on the maintenance of the electron beams after triggering the Type III radio bursts rather than the formation of the beams before the triggering, and the common origin of the electron beams is poorly understood.

It is well known that solar flares accelerate electrons to a power-law energy distribution [12–14] in the magnetic reconnection (MR) region. Theory and particle-in-cell simulations show that the power-law energetic electrons can be produced in the diffusion region of MR [15–17]. However, the bulk velocity of the energetic electrons does not usually exceed the thermal velocity of

Content from this work may be used under the terms of the Creative Commons Attribution 3.0 licence. Any further distribution of this work must maintain attribution to the author(s) and the title of the work, journal citation and DOI.

2544 (2023) 012004

doi:10.1088/1742-6596/2544/1/012004

the electrons due to intense plasma heating in the acceleration region. As a result, energetic electrons cannot trigger the electron two-stream instability (ETSI) immediately and hence do not produce Type III radio bursts in the acceleration region [3,17]. Observations also found that as the energetic electrons continue propagating a certain distance away from the acceleration region, Type III radio bursts are produced [5,6,18–21]. Hence the height of the MR acceleration region where energetic electrons are produced initially is lower than the site where the Type III radio bursts are excited, suggesting that energetic electrons with power-law energy spectra develop into electron beams after they escape from the acceleration region and propagate up along magnetic field lines.

What effects commonly govern the electron beam formation in the solar corona is unclear. The electron Coulomb collision rate in the inner corona is $\nu_{\rm e} \sim 10^{-6} n_{\rm e} T_{\rm e} \sim 10^{-4} {\rm \ s^{-1}}$ and the Coulomb heating timescale is about 10⁴ s. During this period, keV electrons (with a typical velocity about 1×10^3 km/s) travels 100 solar radii. Thus, the impact of Coulomb collisions on the transport of energetic electrons is negligible [22, 23]. Turbulent acceleration is another significant effect [5], but our knowledge about solar corona turbulence is poor, and its origin and intensity are uncertain. One certain effect that can affect electrons along the magnetic field is the magnetic field gradient. The open magnetic field lines forming during magnetic reconnection are highly curved and decrease as they extend from the lower corona to space [24]. Since the magnetic fields of magnetic loops change slowly in time and space compared to the time scale of electrons traveling in the corona, the magnetic moment of the electrons is approximately conserved [25]. Consequently, the conservation of electron magnetic momentum leads to a increased parallel velocity and a decreased perpendicular velocity simultaneously, dubbed as the magnetic focusing effect. Magnetic focusing is an intrinsic feature of the solar magnetic field and can impact the transport of particles throughout the whole solar corona and solar wind. It has been well known that the magnetic focusing effect plays an decisive role in the formation of the solar wind electron strahl at 1 AU, but its role in the development of the fast electron beams within a far-more shorter distance ($\sim 0.002 \text{ AU}$) in the corona has not been well studied.

In this paper, using kinetic transport theory, we show that magnetic focusing effectively transfers the perpendicular momentum to the forward parallel momentum when energetic electrons run away from the acceleration region of solar flares and move up along magnetic field lines. For the first time, we find that the bulk velocity of energetic electrons (electron beam) increases rapidly over a small distance of less than 0.4 solar radii (300 Mm) to much higher than the local electron thermal velocity, indicating that an ETSI can be triggered and a Type III radio burst produced. This result is consistent with observations that observations that the electron beams that produce type III radio bursts are usually found above 100 Mm above photosphere. In a more rapidly decreasing magnetic field, energetic electrons with a harder spectra can develop a faster beam, which triggers the ETSI and produce type III radio bursts at a location much closer to the acceleration region. The spectral index of the power-law energy distribution remains the same as that initially inside the acceleration region.

2. Theoretical model

We modify the gyrophase averaged kinetic transport equation for a gyrotropic electron distribution function $f(\boldsymbol{x}, v, \mu, t)$ [26] to include drift along a general form magnetic field:

2544 (2023) 012004

doi:10.1088/1742-6596/2544/1/012004

$$\frac{\partial f}{\partial t} + (v\mu \boldsymbol{b} + \boldsymbol{U}) \cdot \nabla f
+ \left[\left(-\frac{\partial \boldsymbol{U}}{\partial t} - \boldsymbol{U} \cdot \nabla \boldsymbol{U} \right) \cdot \boldsymbol{b} \frac{\mu}{v} - \frac{1 - \mu^{2}}{2} \nabla \cdot \boldsymbol{U} - \frac{3\mu^{2} - 1}{2} \boldsymbol{b} \cdot \nabla \boldsymbol{U} \cdot \boldsymbol{b} + \frac{qE_{\parallel}\mu}{mv} \right] v \frac{\partial f}{\partial v}
+ \frac{1 - \mu^{2}}{2} \left[v \nabla \cdot \boldsymbol{b} + \mu \nabla \cdot \boldsymbol{U} - \left(\frac{\partial \boldsymbol{U}}{\partial t} + \boldsymbol{U} \cdot \nabla \boldsymbol{U} \right) \cdot \boldsymbol{b} \frac{2}{v} - 3\mu \boldsymbol{b} \cdot \nabla \boldsymbol{U} \cdot \boldsymbol{b} + \frac{2qE_{\parallel}}{mv} \right] \frac{\partial f}{\partial \mu}
= \left(\frac{\delta f}{\delta t} \right)_{sc}$$
(1)

where \boldsymbol{x} is the position in the rest frame, (v, μ) the velocity magnitude and the cosine of pitch angle measured in a moving frame drifting with $\boldsymbol{U} = c(\boldsymbol{E} \times \boldsymbol{B})/B^2 + U_{\parallel}\boldsymbol{b}$ with respect to the rest frame of the Sun, where $U_{\parallel} = \boldsymbol{U} \cdot \boldsymbol{b}$, \boldsymbol{E} and \boldsymbol{B} are the external fields, and $\boldsymbol{b} \equiv \boldsymbol{B}/B$ the unit vector of along the magnetic field. E_{\parallel} and $(\delta f/\delta t)_{\rm sc}$ are the parallel electric field and scattering mechanisms, and both are ignored in the present paper since magnetic focusing alone is considered.

Consider a constant drifting velocity of the moving frame along the magnetic field U = Ub, it is easy to show that $\nabla \cdot U = U\nabla \cdot b$. The derivative divergence of b can be expressed in terms of the magnetic field B:

$$\nabla \cdot \boldsymbol{b} = -\frac{\boldsymbol{B} \cdot \nabla B}{B^2}.\tag{2}$$

where $\nabla \cdot \boldsymbol{B} = 0$ has been taken into consideration. In a global spherical coordinate system whose origin is the center of the Sun, let $\mathbf{B} = B_r \hat{e}_r + B_\theta \hat{e}_\theta + B_\phi \hat{e}_\phi$, where \hat{e}_r , \hat{e}_θ and \hat{e}_ϕ are the radial, polar and azimuthal unit vectors, respectively. We are interested in the outward transport of energetic electrons in solar flares. For the solar flare background, the magnetic loops are approximately force-free, and the magnetic field model proposed by Antiochos et al. [24] is commonly accepted. In this model, it is assumed that the radial component is much larger than the other two components, i.e., $B \approx B_r$ [24]. The divergence of \boldsymbol{b} becomes:

$$\nabla \cdot \boldsymbol{b} \approx -\frac{\partial \ln B}{\partial r},\tag{3}$$

where r is the radial distance. The velocity v of electrons is always much larger than the plasma background velocity U, i.e., $U \ll v$, making it safe to ignore U. Therefore, the transport equation (1) reduces to:

$$\frac{\partial f}{\partial t} + \mu v \frac{\partial f}{\partial r} - \frac{1}{2} \frac{d \ln B}{dr} (1 - \mu^2) v \frac{\partial f}{\partial \mu} = 0.$$
 (4)

Compared with equation (1), the magnetic field in equation (4) is restricted to a magnetic field configuration whose non-radial components are much weaker than radial. As a result, the effect of focusing by the non-radial components of the magnetic field is negligible, and thus the distribution function f is nearly independent of θ and ϕ in the global spherical coordinate system. Therefore, in the following, we only consider the radial magnetic field.

The magnetic field of a solar flare varies with time, and its timescale is much larger than that of energetic electrons transport in the solar corona. For example, a 10 keV electron whose velocity is about 10⁴ km/s needs 10 s to travel one solar radius, which is much shorter than the 1000 s time scale of a typical solar flare [6]. Hence it is reasonable to assume that energetic

2544 (2023) 012004

doi:10.1088/1742-6596/2544/1/012004

electrons experience an approximately "stationary" magnetic field as they transport in the solar corona—this is the condition for the conservation of magnetic moment, which causes magnetic focusing in a spatially decreasing magnetic field. As a magnetic field decreases with radial distance r, the simplest case is $B = B_0/r^2$, which ensures the divergence-free condition of magnetic field, otherwise, the magnetic field must include the other two components but they are assumed to be sufficiently small compared to the radial component and can be safely ignored. To choose the radial magnetic field configuration, we follow the reference scenario in the modeling of solar magnetic field by Banaszkiewicz et al. [27] and open magnetic field lines of solar flares by Antiochos et al. [24]. We approximate the outward magnetic field lines of the solar flares as $B = B_0/r^{n_{\rm B}}$, where B_0 is the magnetic field at the inner boundary, $n_{\rm B} = 1, 2, 3, \cdots$. A more general form of the magnetic field can be expressed as a summation of a series of $1/r^{n_{\rm B}}$. With this configuration, we can understand how the spatial evolution of the magnetic field impacts magnetic focusing and the resulting beam development. Hence, $d \ln B/dr = -n_{\rm B}/r$ and only the value of $n_{\rm B}$ enters in the transport equation (4) while the exact value of the magnetic field disappears:

$$\frac{\partial f}{\partial t} + \mu v \frac{\partial f}{\partial r} + \frac{n_{\rm B}}{2} \frac{(1 - \mu^2)v}{r} \frac{\partial f}{\partial \mu} = 0.$$
 (5)

The energetic electron VDF produced at the acceleration region of MR is used as the initialization at the inner boundary. A combination of a drifting Maxwellian $(f_{\rm m})$ and a drifting power-law $(f_{\rm p})$ is chosen to mimic the energetic electron VDFs with a drifting velocity $U_{\rm d}$. Hence,

$$f(v, \mu \ge 0) = \delta f_{\rm m}(v, \mu) + (1 - \delta) f_{\rm p}(v, \mu),$$
 (6)

$$f_{\rm m}(v,\mu) = n_0 \left(\frac{m}{2\pi k_{\rm B} T_{\rm c0}}\right)^{3/2} \exp\left\{-\frac{m}{2k_{\rm B} T_{\rm c0}} \left[(v\mu - U_{\rm d})^2 + v^2 \left(1 - \mu^2\right) \right] \right\},\tag{7}$$

$$f_{\rm p}(v,\mu) = n_0 \frac{1}{4\pi} \frac{\alpha - 3}{v_{\rm c}^{3-\alpha}} \left\{ \left[(v\mu - U_{\rm d})^2 + v^2 (1 - \mu^2) \right]^{1/2} \right\}^{-\alpha}, \quad (v\mu - U_{\rm d})^2 + v^2 (1 - \mu^2) \ge v_{\rm c}^2.$$
(8)

where δ is the weight of the Maxwellian component $f_{\rm m}$, $T_{\rm c0}$ the temperature of the Maxwellian component, n_0 the total electron number density at the inner boundary, $v_{\rm c}$ the critical velocity separating the power-law component (energetic electrons) from the Maxwellian, and α the spectral index of the power-law component. The upper-left panel in Figure 1 shows an example of the electron VDF at the inner boundary in the $(v_{\parallel}, v_{\perp})$ plane in the case of $\delta = 0.8$, $\alpha = 4$, $U_{\rm d} = 1v_{\rm th0}$ and $n_{\rm B} = 2$.

We numerically solve the transport equation (5) with boundary condition (6) - (8) to study the transport of energetic electrons in the corona from 1.05 to 3.05 $R_{\rm s}$, where $R_{\rm s}$ is the solar radius. The inner boundary of 1.05 $R_{\rm s}$ is chosen by assuming the accelerated electrons are injected in the acceleration region of MR, which is in the lower corona [5,19,28], and the outer boundary of 3.05 $R_{\rm s}$ is the typical size of magnetic loops [24]. We choose the critical velocity $v_{\rm c}=1.5v_{\rm th0}$, where $v_{\rm th0}=(2k_BT_{\rm c0}/m)^{1/2}$ is the electron thermal velocity at the inner boundary. We adjust the parameters α and $U_{\rm d}$ to mimic the diverse power-law electron energy spectra and the drifts of electron outflows produced by MR acceleration. We adjust $n_{\rm B}$ to mimic the open field lines in MR produced by magnetic field lines with different curvatures. The various combinations of different α , $U_{\rm d}$ and $n_{\rm B}$ used in the calculation are listed in Table 1 and the meaning will be explained and discussed in detail in the following sections. The numerical stationary solution is obtained after the code approaches the steady final state.

2544 (2023) 012004

doi:10.1088/1742-6596/2544/1/012004

Table 1. Combinations of different Parameters
--

α	$U_{ m d}(v_{ m th0})$	$n_{ m B}$
4	0	3
4	1	1
4	1	2
4	1	3
4	1	5
4	0.5	3
6	0.5	3
8	0.5	3

3. Numerical results

Magnetic focusing is the direct consequence of the conservation of magnetic moment defined as $\mu_M = mv_{\perp}^2/2B$. The magnetic field decreases as the electrons move outward along open magnetic field lines. The conservation of μ_M results in a decrease of the perpendicular electron velocity, and conservation of electron kinetic energy increases the parallel electron velocity.

The steady analytical solution $f(r, v, \mu)$ of equation (5) can be obtained by the method of characteristics [29, 30]:

$$f(r, v, \mu) = \begin{cases} f_0(r_0, v, \mu), & \sqrt{1 - \left(\frac{r_0}{r}\right)^{n_B}} < \mu < 1 \\ 0. & -1 < \mu < \sqrt{1 - \left(\frac{r_0}{r}\right)^{n_B}} \end{cases},$$
(9)

where $f_0(r_0, v, \mu)$ is any given inner boundary condition r_0 . Figure 1 shows the numerical solution for the radial evolution of the electron VDF at 1.05, 1.5, 2 and 3 $R_{\rm s}$ respectively, for a velocity distribution with $\delta=0.8$, $\alpha=4$, $U_{\rm d}=1v_{\rm th0}$ and $n_{\rm B}=2$ at the inner boundary. As distance increases, the electron VDFs become increasing anisotropic, i.e., the maximum pitch-angle of the electron VDF decreases with the increasing distance, which is due to focusing induced by a decreasing magnetic field, the maximum value of the electron perpendicular velocity decreases while that of the parallel velocity increases, leading to the formation of a group of fast outward-moving electrons - an electron beam.

To study the radial evolution of the bulk velocity of energetic electrons, we define it as:

$$u_{\rm b} = \frac{2\pi \int_{v_{\rm min}(r,\mu)}^{\infty} dv \int_{\mu_{\rm min}(r)}^{1} d\mu v^{3} \mu f}{2\pi \int_{v_{\rm min}(r,\mu)}^{\infty} dv \int_{\mu_{\rm min}(r)}^{1} d\mu v^{2} f}.$$
 (10)

This definition is similar to the definition of the mean electron velocity within the beam [7]. Hence, $\mu_{\min}(r) = \sqrt{1 - \left(r_0/r\right)^{n_{\rm B}}}$ is the cosine of the maximum pitch-angle of the electron VDF at distance r, which is given by the analytical solution (9). At r_0 , $\mu_{\min} = 0$, and increases with increasing distance and $v_{\min} = U_{\rm d}\mu + \sqrt{U_{\rm d}^2(\mu^2 - 1) + v_{\rm c}^2}$ is the critical velocity of the power-law

2544 (2023) 012004

doi:10.1088/1742-6596/2544/1/012004

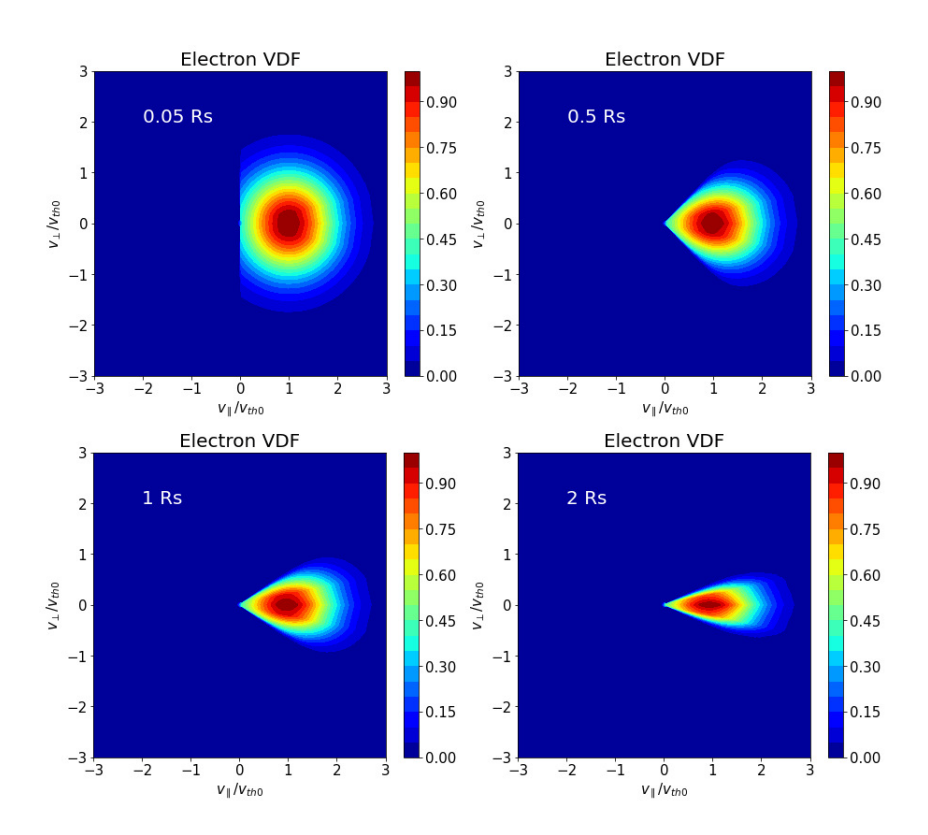


Figure 1. 2D contour plots of the electron VDF in the moving frame at 1.05, 1.5, 2 and 3 $R_{\rm s}$ for $U_{\rm d}=1v_{\rm th0}$ and $B=B_0/r^2$.

component, for which $v_{\min} = v_c$ if $U_d = 0$. In the case of $U_d \neq 0$, $f(r, v, \mu)$ and v_{\min} are highly anisotropic, and the analytical solution of u_b is hard to obtain.

The radial evolution of the bulk velocity of the energetic electron $u_{\rm b}$ in the rest frame of the Sun is shown in Figure 2, A1 and A2. Figure 2 A1 has a Maxwellian velocity distribution with weight $\delta=1$ at the inner boundary. In Figure 2 A2 the electron VDF at the inner boundary is a Maxwellian with weight $\delta=0.8$ plus a power-law velocity tail (energetic electrons) with index $\alpha=4$ and weight 0.2 (= $1-\delta$). The index $\alpha=4$ is estimated according to the lower bound of the observable index of electron energy spectra which is about 3 [6,18,31,32], and the weight 0.2 (= $1-\delta$) is estimated by the typical acceleration efficiency found in PIC simulations [16,17]. Different velocity starting points of $u_{\rm b}$ are caused by the different drifting velocities $U_{\rm d}$ (0, $0.5v_{\rm th0}$ and $v_{\rm th0}$) of the electron VDF at the inner boundary.

It can be seen that $u_{\rm b}$ under all conditions increases sharply from the inner boundary 1.05 to 1.4 $R_{\rm s}$ (i.e., over a distance of 0.4 $R_{\rm s}$, or 300 Mm), indicating that magnetic focusing increases the parallel bluk velocity when energetic electrons move upward along magnetic field lines. Comparing with A1, Figure 2 A2 shows that the energetic electrons with a power-law energy spectrum escaping from the acceleration region can be more efficiently focused to reach a higher bulk velocity, which is about three times larger than the thermal velocity $v_{\rm th0}$. The decreasing electron temperature with distance in the corona leads to a decrease of the local electron thermal velocity ($v_{\rm th0} > v_{\rm th}$). Therefore above a distance of 0.4 $R_{\rm s}$ (300 Mm), energetic electrons likely have a bulk velocity $u_{\rm b}$ that is a much larger value than the local electron thermal velocity, i.e. $u_{\rm b} \gg v_{\rm th}$. These energetic electrons with large bulk velocity can trigger a strong ETSI and produce Type III radio bursts [3, 33], which is consistent with the observations that type III radio bursts are always found above a certain distance (> 300 Mm) from the acceleration

2544 (2023) 012004

doi:10.1088/1742-6596/2544/1/012004

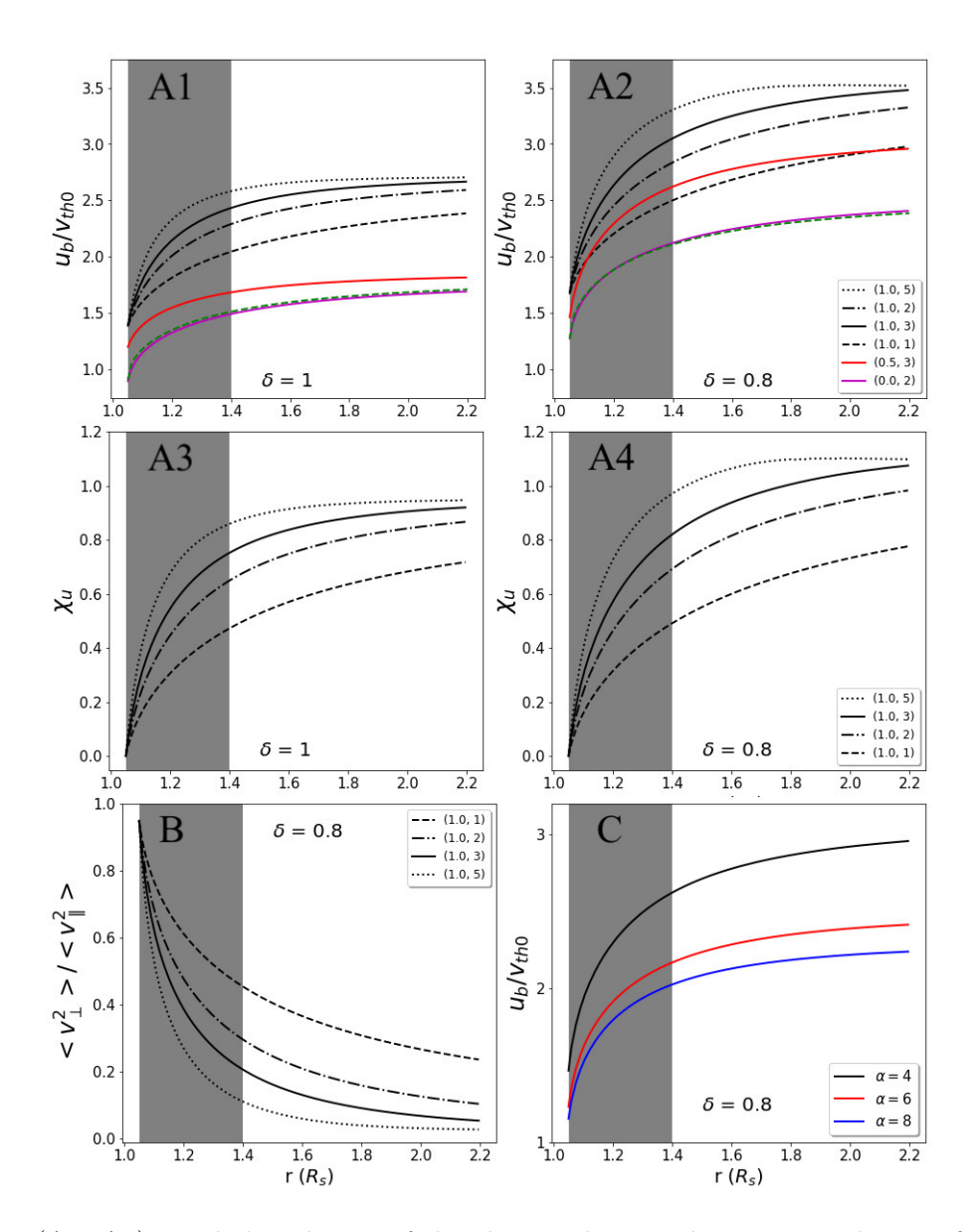


Figure 2. (A1, A2): Radial evolution of the electron beam velocity $u_{\rm b}$ in the rest frame. A1: The inner boundary condition of the electron VDF is an isotropic Maxwellian only. A2: The inner boundary condition of the electron VDF is an isotropic Maxwellian with weight $\delta=0.8$ plus an isotropic power-law with $\alpha=4$ and weight 0.2 (= 1 - δ). The drifting velocity $U_{\rm d}$ and $n_{\rm B}$ of magnetic field $B=B_0/r^{n_{\rm B}}$ are shown in the brackets ($U_{\rm d}, n_{\rm B}$). (A3, A4): Radial evolution of electron beam velocity growth rate χ_u corresponding to A1 and A2 respectively. B: Radial evolution of $< v_{\perp}^2 > / < v_{\parallel}^2 >$ for an electron beam. Line colors and styles have the same meaning as in A2. C: Radial revolution of $u_{\rm b}$ with different power-law indices $\alpha=4$, 6 and 8. The shaded areas indicate the distance range from 1.05 to 1.4 $R_{\rm s}$.

region [19, 20]. We find that even though the hot electrons do not develop outflow in the acceleration region, the energetic electrons can escape and generate a bulk flow with velocity $u_{\rm b}$ much larger than the electron thermal velocity $v_{\rm th0}$, and trigger ETSI.

The differences between Figure 2 A2 and A1 illustrate how the magnetic field and power-law tail affect the increase in the bulk velocity of the energetic electrons. First, the bulk velocity

2544 (2023) 012004

doi:10.1088/1742-6596/2544/1/012004

 $u_{\rm b}$ in A2 has a higher initial value at the inner boundary and a higher final value at the outer boundary than those in A1. The power-law tail in A2 provides more energetic electrons, leading to a higher initial $u_{\rm b}$. To study the increased efficiency, we define a growth rate for the electron bulk velocity as $\chi_u = (u_{\rm b} - u_{\rm b0})/u_{\rm b0}$ where $u_{\rm b0}$ is the initial $u_{\rm b}$ at the inner boundary. The radial evolution of the growth rates χ_u are shown in A3 and A4 in Figure 2, where A3 is derived from A1 and A4 from A2. The growth rates χ_u in A4 are larger than those in A3, showing that magnetic focusing of electrons with a power-law tail leads to a higher bulk velocity than the case of a Maxwellian distribution only. Therefore magnetic focusing can increase the electron bulk velocity much more rapidly if more energetic electrons with a power-law tail are present, thus triggering ETSI and producing type III radio bursts. Second, the $n_{\rm B}$ in magnetic field $B = B_0/r^{n_{\rm B}}$ also affects the radial evolution of $u_{\rm b}$ and its growth rate χ_u . As $n_{\rm B}$ increases from $n_{\rm B} = 1$ to 3, and to 5, both the electron bulk velocity $u_{\rm b}$ and its growth rate χ_u increase faster and reach a larger value. Consequently, in a more rapidly decreasing magnetic field, we expect more Type III radio bursts to occur at distances closer to the acceleration region of MR.

Magnetic focusing causes the parallel acceleration of electrons along the magnetic field line by transferring electron kinetic energy from the perpendicular direction to the parallel direction. We calculate the ratio of the perpendicular kinetic energy to the parallel kinetic energy of electrons $(\langle v_{\perp}^2 \rangle / \langle v_{\parallel}^2 \rangle)$ using

$$\frac{\langle v_{\perp}^2 \rangle}{\langle v_{\parallel}^2 \rangle} = \frac{\int_0^{\infty} v_{\perp}^2 f d\boldsymbol{v}}{\int_0^{\infty} v_{\parallel}^2 f d\boldsymbol{v}}.$$
 (11)

Figure 2B displays the radial evolution of the kinetic energy ratio in the A2 case with $\delta=0.8$ and $U_{\rm d}=v_{\rm th0}$. We find that the kinetic energy ratios start from less than 1 and decrease with distance. For an isotropic electron VDF at the inner boundary, the kinetic energy ratio is 2 since the isotropic VDF has one degree of freedom in the parallel direction and two in the perpendicular direction. However, in our case, the electron VDF with a drifting velocity $U_{\rm d}\neq 0$ is anisotropic, and its kinetic energy ratio is less than 2. The radial evolution of the kinetic energy ratio decreases with distance which contrasts with the radial evolution of the electron bulk velocity $u_{\rm b}$ and its growth rate χ_u . It is noticeable that the kinetic energy ratio decreases sharply in the same distance range from 1.05 to 1.4 $R_{\rm s}$, while $u_{\rm b}$ and χ_u , on the contrary, increase sharply. The radial evolution of kinetic energy ratio caused by the magnetic focusing effect is dominated by the value of $n_{\rm B}$ in $B=B_0/r^{n_{\rm B}}$: the larger $n_{\rm B}$, the faster the decrease of kinetic energy ratio.

Panel C of Figure 2 shows the radial evolution of electron beam velocity $u_{\rm b}$ of electrons with different energy spectral indices α . The electron bulk speed $u_{\rm b}$ with a smaller spectral index α has a higher initial value since the electron VDF with a smaller spectral index α possesses more energetic electrons. The smaller spectral index α leads to a faster increase of $u_{\rm b}$ with radial distance. Similarly, the maximum increase is in the same gray-shaded area.

We find that the electron energy spectral index α of energetic electrons is preserved during the upward propagation in the presence of magnetic focusing. We plot a parallel cut of the electron VDF $(v_{\parallel} > 0)$ in Figure 3 and consider the radial evolution of the energy spectra index α of the power-law tail. The energy spectral index α does not change with distance, and the more distant electron VDF in interplanetary space has the same index α as the electron VDF at the inner boundary. Consequently, the information embedded in the distribution function of the energetic electrons produced in the acceleration region of the solar flare is preserved.

2544 (2023) 012004

doi:10.1088/1742-6596/2544/1/012004

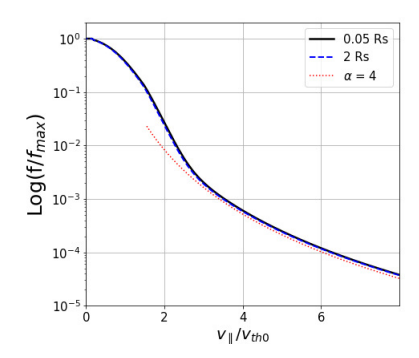


Figure 3. A parallel cut of the electron VDFs at the inner and outer boundary. The normalized electron VDF is calculated as f/f_{max} where f_{max} is the maximum. At $v_{\parallel} > 0$, the outwardly propagating electron VDFs overlap and both have $\alpha = 4$.

4. Discussion and conclusion

Observations of coronal Type III radio bursts discovered that electron beams are commonly produced in solar flares [6,8,34], and the location of these beams is beyond some 300 Mm from the acceleration region. However, the origin of electron beams is poorly understood. In this paper, we investigate the transport of energetic electrons produced in the acceleration region of solar flares as they propagate upward along the magnetic field lines of a solar flare. Magnetic focusing is an intrinsic property of a decreasing strength magnetic field, typical of the solar corona and solar wind, which transfers electron perpendicular momentum and kinetic energy to the parallel direction. We ignore Coulomb and wave-particle scattering terms and construct a kinetic transport equation for energetic electrons in the solar corona subject to magnetic focusing. By numerically solving the kinetic transport equation, we investigate how magnetic focusing affects the transport of energetic electrons along outward magnetic field lines in the solar corona. Observations established that electrons are commonly accelerated by solar flares to power-law energy spectra in the acceleration region. Here we mimic the acceleration process by choosing the initial eVDF at the inner boundary with a power-law tail, and the power-law index range varies from 4 to 8, consistent with the observations.

We find that the magnetic focusing effect sharply increases the bulk velocity of energetic electrons over an observational desired distance of less than 0.4 solar radii (300 Mm) to be much larger than the local electron thermal velocity. Energetic electrons with bulk velocity much larger than the local electron thermal velocity can trigger type III radio bursts. This is consistent with observations that the electron beams that produce type III radio bursts are usually found above 300 Mm above photosphere. In a more rapidly decreasing magnetic field (larger $n_{\rm B}$), energetic electrons with a harder power-law energy spectrum (smaller α) can drive a faster beam. Energetic electrons with higher bulk velocity can trigger the ETSI and produce type III radio bursts at a location much closer to the acceleration region. Magnetic focusing does not change the initial spectral index α of energetic electrons as they propagate outward along magnetic field lines. Thus, outwardly moving energetic electrons preserve the electron distribution information from the region where they initially formed.

This paper focuses on the magnetic focusing effect. It will be necessary to extend our numerical model to include Coulomb collisions and turbulence, investigating the competition between these three effects in forming electron beams. This will be presented in a following paper.

Acknowledgment. B. T. and H. C. acknowledge partial support by NASA HSR program No. 80NSSC21K0031, a Heliophysics Career award No. 80NSSC19K1106, and NSF CAREER 2144324. The authors acknowledge the partial support of an NSF EPSCoR RII-Track-1

2544 (2023) 012004 doi:10.1088/1742-6596/2544/1/012004

Cooperative Agreement OIA-2148653.

References

- [1] Wild J and McCready L 1950 Australian Journal of Chemistry 3 387–398
- [2] Aschwanden M J 2002 Particle acceleration and kinematics in solar flares 1–227
- [3] Che H 2016 Modern Physics Letters A **31** 1630018
- [4] Ginzburg V and Zhelezniakov V 1958 Soviet Astronomy 2 653
- [5] Reid H A, Vilmer N and Kontar E P 2011 Astronomy & Astrophysics 529 A66
- [6] Benz A O 2017 Living Reviews in Solar Physics 14 1–59
- [7] Reid H A and Kontar E P 2018 The Astrophysical Journal 867 158
- [8] Saint-Hilaire P, Vilmer N and Kerdraon A 2012 The Astrophysical Journal 762 60
- [9] Che H and Goldstein M 2014 The Astrophysical Journal Letters 795 L38
- [10] Che H, Goldstein M, Salem C and Viñas A 2019 The Astrophysical Journal 883 151
- [11] Li B, Robinson P A and Cairns I H 2006 Physical Review Letters 96 145005
- [12] Krucker S, Oakley P and Lin R 2009 The Astrophysical Journal 691 806
- [13] Lin R 2011 Space science reviews 159 421
- [14] Zharkova V V, Arzner K, Benz A O, Browning P, Dauphin C, Emslie A G, Fletcher L, Kontar E P, Mann G, Onofri M et al. 2011 Space science reviews 159 357
- [15] Zank G, Le Roux J, Webb G, Dosch A and Khabarova O 2014 The Astrophysical Journal 797 28
- [16] Che H and Zank G 2020 The Astrophysical Journal 889 11
- [17] Che H, Zank G, Benz A, Tang B and Crawford C 2021 The Astrophysical Journal 908 72
- [18] Krucker S, Kontar E, Christe S and Lin R 2007 The Astrophysical Journal Letters 663 L109
- [19] Chen B, Bastian T S, White S M, Gary D E, Perley R, Rupen M and Carlson B 2013 The Astrophysical Journal Letters 763 L21
- [20] Chen B, Yu S, Battaglia M, Farid S, Savcheva A, Reeves K K, Krucker S, Bastian T, Guo F and Tassev S 2018 The Astrophysical Journal 866 62
- [21] Benz A O 2012 Plasma astrophysics: Kinetic processes in solar and stellar coronae vol 184 (Springer Science & Business Media)
- [22] Fuchs V, Cairns R, Lashmore-Davies C and Shoucri M 1986 The Physics of fluids 29 2931–2936
- [23] Berčič L, Landi S and Maksimović M 2021 Journal of Geophysical Research: Space Physics 126 e2020JA028864
- [24] Antiochos S, DeVore C, Karpen J and Mikić Z 2007 The Astrophysical Journal 671 936
- [25] Marsch E 2006 Living Reviews in Solar Physics 3 1
- [26] Zank G P 2014 Transport Processes in Space Physics and Astrophysics (Lecture Notes in Physics, Berlin Springer Verlag vol 877) (Springer-Verlag)
- [27] Banaszkiewicz M, Axford W and McKenzie J 1998 Astronomy and Astrophysics 337 940–944
- [28] Cairns I H, Lobzin V, Donea A, Tingay S, McCauley P, Oberoi D, Duffin R, Reiner M, Hurley-Walker N, Kudryavtseva N et al. 2018 Scientific reports 8 1–12
- [29] Sone Y and Sugimoto H 1993 Physics of Fluids A: Fluid Dynamics 5 1491–1511
- [30] Tang B, Zank G P and Kolobov V I 2020 The Astrophysical Journal 892 95
- [31] Lin R, Evans L and Fainberg J 1973 Astrophysical Letters 14 191
- [32] Lin R, Potter D, Gurnett D and Scarf F 1981 The Astrophysical Journal 251 364–373
- [33] Che H, Goldstein M L, Diamond P H and Sagdeev R Z 2017 Proceedings of the National Academy of Sciences 114 1502–1507
- [34] Reid H A S and Ratcliffe H 2014 Research in Astronomy and Astrophysics 14 773